PIERCE DIODE WITH EXTERNAL CIRCUIT. III. CHAOTIC BEHAVIOR

by

William S. Lawson

Memorandum No. UCB/ERL M87/74

28 October 1987

PIERCE DIODE WITH EXTERNAL CIRCUIT. III. CHAOTIC BEHAVIOR

by

William S. Lawson

Memorandum No. UCB/ERL M87/74

28 October 1987

ELECTRONICS RESEARCH LABORATORY

College of Engineering
University of California, Berkeley
94720

PIERCE DIODE WITH EXTERNAL CIRCUIT. III. CHAOTIC BEHAVIOR

by

William S. Lawson

Memorandum No. UCB/ERL M87/74

28 October 1987

ELECTRONICS RESEARCH LABORATORY

College of Engineering
University of California, Berkeley
94720

PIERCE DIODE WITH EXTERNAL CIRCUIT. III. CHAOTIC BEHAVIOR

William S. Lawson

28 October 1987

Abstract

The existence of the strange attractor discovered by Godfrey in the neighborhood of $\alpha = 3\pi$ for the Pierce Diode is verified, and his numerical results are refined. The evolution of this attractor is then followed as an external capacitance is introduced.

Introduction

The Pierce diode is perhaps the simplest realistic theoretical model for a bounded one-dimensional plasma system. It is comprised of two parallel electrodes with electrons injected at one of the electrodes with velocity v_0. Ions are considered to be infinitely massive, and in a uniform background which neutralizes the charge density of the electrons at the electrode from which the electrons are injected. The electrodes are also held at the same potential, *i.e.*, short-circuited (see Fig. 1). This short circuit allows feedback, and leads to a wealth of interesting behavior. The Pierce diode is completely characterized by a single dimensionless parameter $\alpha = \omega_p L/v_0$ where ω_p is the plasma frequency of the electron beam, and L is the distance between the electrodes [1].

One interesting feature of the Pierce diode which was discovered by Godfrey [2], is that for a narrow range of the parameter α, the Pierce diode exhibits chaotic behavior without violent disruption (violent disruption meaning virtual cathode formation and the return of electrons to the emitter). This behavior was observed through simulations in the neighborhood of $\alpha = 2.85\pi$, and it is believed to recur approximately at intervals of 2π. The observed behavior includes a Hopf bifurcation followed by period doubling bifurcations leading to chaotic behavior following the scenario described by Feigenbaum [3]. The reason for the formation of the observed strange attractor is uncertain, but its sudden disappearance is associated with a near-by unstable equilibrium state.

The extended Pierce diode is similar to the standard (or classical) Pierce diode, but instead of a short circuit between the bounding electrodes, a series RLC circuit is used (see Fig. 2). The behavior of the extended Pierce diode in the linear regime has been worked out [4] and verified through simulation [5], and its non-uniform equilibria have also been investigated [6]. In the work which

follows, I shall not consider the effect of varying the external resistor or inductor, but will vary only the external capacitance. The external capacitance has the most profound effect on the non-uniform equilibria of the extended Pierce diode (indeed it is the only external circuit element to affect the equilibria), and thus should be the first parameter varied in exploring the strange attractor.

General Properties of the Pierce Diode Equations

The equations of evolution for the Pierce diode with an external capacitor have been derived elsewhere [6]. They are

$$T(t) = 1 - \frac{1}{\alpha}\int_{t-T}^{t} E(\tau)\sin\alpha(t-\tau)\,d\tau \tag{1}$$

and

$$\left(1+\frac{1}{C}\right)E(t) = \frac{\alpha^2}{2}\left(1-T(t)^2\right) - \alpha\int_{t-T}^{t} E(\tau)(t-\tau)\sin\alpha(t-\tau)\,d\tau \tag{2}$$

where $T(t)$ is the transit time of the electrons just leaving at time t, and $E(t)$ is the electric field at the injection plane at time t. These equations have several properties which are not obvious, and these will be discussed. One important property which is not yet known is whether this equation is reversible in time; specifically, given $E(t)$ over a transit time, is $E(t)$ is unique for earlier times than those given. This question is of great importance in understanding the character and origin of the strange attractor. Evidence will be presented for both sides of this question, but a definitive answer is not yet known.

The most obvious property of this equation is that it is not what is usually called an equation of evolution, since the formulas do not specify time derivatives of the variables, but rather the variables themselves. This simplifies the numerical solution of the equations, but complicates the issue of reversibility. Another fundamental property of the equations is that $T(t)$ is purely an auxiliary variable; given $E(t)$ over a long enough initial time (long enough for the electron emitted at the earliest time to have exited), $T(t)$ can be computed for any time at which it is needed.

A less obvious property of these equations is that perfectly valid initial conditions for the *physical* problem cannot always be translated into initial conditions for these equations. Consider, for example, the perfectly reasonable condition of sinusoidally perturbed positions, and uniform velocities, *i.e.*, $v(x) = 1$ and $x(t_0) = t - t_0 + \epsilon\sin kt$ (I shall use dimensionless variables throughout this article). The equations for x and v as functions of t and t_0 (from [6]) are

$$x = t - t_0 + \frac{1}{\alpha}\int_{t_0}^{t} E(\tau)\sin\alpha(t-\tau)\,d\tau \tag{3}$$

and

$$v = 1 + \int_{t_0}^{t} E(\tau)\cos\alpha(t-\tau)\,d\tau \tag{4}$$

If $v = 1$ for all t_0, then plainly, $E(\tau) = 0$ for all $\tau < t$. This precludes the desired perturbation in position, however. Thus this initial situation could not have come about from the evolution of the system, and the full fluid equations must be used to advance the system for one complete transit time before Godfrey's integral equations can be applied. This in turn would seem to implies some loss of information, and some irreversibility over at least the first transit time.

The loss of information is more obvious from the simple consideration that in choosing the initial conditions, one can choose $\rho(x)$ and $v(x)$ without constraint, whereas in choosing the initial conditions for Godfrey's equations, only one function, $E(t)$ may be chosen. Thus it is impossible to run the integral equations backwards to reproduce an arbitrary initial condition, since not enough information is present.

There is no strong reason to expect more loss of information after one transit time, though, since after a transit time, all the electrons in the system are subject to the constraint that at their time of injection, $\rho = v = 1$. This imposes a constraint between ρ and v which did not exist in the initial conditions. This constraint is enough to guarantee that ρ and v can be reconstructed from $E(t)$. This loss of information can clearly be seen in Fig. 3 which shows a phase space plot for a Pierce diode which was loaded with random perturbations in position. The potential behind the last of the initially-loaded particles is smooth, but the potential ahead of it is still quite noisy. To summarize, the complete fluid equations are irreversible (due to the loss of particles at uncontrolled velocity and density at the collection plane), but the integral equations, which have an additional constraint, *may* be reversible. The issue of reversibility will be brought up again when the return maps are discussed.

Physical Validity of Solution

For Eqs. (1) and (2) to be *physically* valid, it is necessary for the velocity of the stream of particles to be a single-valued function of position. The situation depicted in Fig. 4a is physically valid, but the integral equations do not correctly model it. Since the velocity is a single-valued function of t_0, it is only necessary for x to be a monotonic (in this case decreasing) function of t_0. From Eq. (3),

$$\frac{dx}{dt_0} = -1 - \frac{1}{\alpha}E(t_0)\sin\alpha(t-t_0) < 0 \tag{5}$$

so physically, it is necessary for

$$E(t_0)\sin\alpha(t-t_0) > -\alpha \tag{6}$$

Since α is large, this implies that whenever

$$|E(t)| < \alpha \tag{7}$$

is violated, the solution will soon become unphysical.

Another situation which is not physically allowed, but can occur in the solution of Eqs. (1) and (2) is that depicted in Fig. 4b. Here, the velocity of the "outgoing" particles has reversed, so that particles which physically would have been absorbed (but which still exist mathematically), are re-entering the region of interest. Again, the Eqs. (1) and (2) allow this without contradiction, even though the situation is unphysical. The simplest test for this situation is that when

$$\frac{dT}{dt} > 1 \tag{8}$$

the solution is no longer physically valid. The transit time T represents the "age" of whatever particle is at the exit plane. If this age is increasing faster than the flow of time, then it must be that particles which were once past the boundary are re-entering.

Mathematically speaking, the physical constraints on the solution are rather arbitrary. Since the solution of Eqs. (1) and (2) may be of *mathematical* interest despite being unphysical, in the work presented here, *all purely physical restrictions have been ignored.* The situations represented in Figs. 4a-d are thus allowed, but Figs. 4c and 4d lead to problems of a mathematical character which dictate the termination of the solution. In Fig. 4c, the particles in the top part of the "S" are affecting the solution even though they have passed beyond the physical boundary of the system, because they were emitted at a time later than $t - T$, and so are still included in both Eq. (1) and Eq. (2). This is mathematically acceptable. The difficulty arises when the lower bend of the "S" moves across the right-hand boundary, and the solution for T (from Eq. (1)) ceases to exist. A new solution could be found, but it would have to jump discontinuously, and since the solution has already lost physical validity, there can be no justification for this.

In Fig. 4d, the opposite problem occurs as in Fig. 4c. Again, the solution for T ceases to exist, and the integration of the equations must stop. Both the situation in Fig. 4c and Fig. 4d occur when dx/dt_0 at the exit plane ($t = t_0 + T$) becomes zero. Thus, from Eq. 5, when

$$1 + \frac{1}{\alpha}E(t-T)\sin\alpha T \rightarrow 0 \tag{9}$$

the integration of the equations must end. *This is the only criterion (other than a time limit) on which the integration was stopped.*

In practice the effect of the physical restrictions is to impose an amplitude limit on the oscillations. This has no effect on the bifurcation diagram for $C = \infty$ (the short circuit case), but as the external capacitance is decreased, the amplitude of the stable oscillations tends to increase, and so part of the high- amplitude end of the bifurcation diagram will be lost.

Numerical Integration Scheme

The integral equations are of non-standard form, and the method of numerical integration used is therefore unusual. As with most methods of time integration, the continuous functions E and T are discretized at uniform time intervals $t_{n+1} = t_n + \Delta t$ so that $E_n \approx E(t_n)$, and similarly for T.

Inspection of Eq. (1) reveals that only the left-hand side of the equation (for $t = t_n$) depends on a quantity known at t_n, since the kernel of the integral vanishes at $\tau = t$. Thus the integral can be evaluated numerically, in order to find T_n (this is a little tricky since the lower integration limit depends on T_n, but some simple algebra solves the problem). This value of T_n can be put into Eq. (2), and the integral in Eq. (2) can be evaluated just as the integral of Eq. (1) was, in order to calculate E_n.

There is a slight difficulty in evaluating the integrals at the lower limit of $\tau = t - T$. Since the transit time T will not be a multiple of the time step Δt, the last interval to be integrated will not be a full time step wide. This fraction of a time step need not be evaluated *as* accurately as the rest of the integral (since the error it produces occurs only once), but it cannot be ignored. If the trapezoidal rule is used for the integration, then linear interpolation of the indefinite integral is sufficiently accurate (some runs with a more sophisticated method of handling the last time step verified this). It is not clear that a higher-order method of integration (*e.g.*, Simpson's Rule) would improve the accuracy of the results, since the derivation of these higher order methods assumes that the function to be integrated is a known, smooth function, whereas our integrand is a discrete approximation.

It is possible to speed up the numerical scheme considerably by expanding $\sin\alpha(t-\tau)$ and writing

$$\int E(\tau)\sin\alpha(t-\tau)\,d\tau = \sin\alpha t \int E(\tau)\cos\alpha\tau\,d\tau - \cos\alpha t \int E(\tau)\sin\alpha\tau\,d\tau \qquad (10)$$

The integrands on the right do not depend on time, and the limits of integration vary slowly with time. This allows the integrals to be computed each time step by adjusting for the small change in the limits of integration rather than recomputing the entire integral. This saves much computer time. This scheme does require that α be strictly constant, which is a problem in generating bifurcation diagrams; however, α can be varied by small jumps after which the integrals on the right-hand side of (10) must be completely re-evaluated. The solution before the jump in α becomes the initial condition on the solution after the jump. If these jumps are infrequent, much computer time can still be saved by using this scheme.

This numerical integration scheme was tested on some equilibrium solutions which are known from theory [2], and the results were accurate to four decimals. It is to be expected that the time-varying solution will be less accurate, but of the same order of accuracy.

As was mentioned in the previous section, the integration must be stopped when condition (9) occurs. Not surprisingly, the left-hand side of Eq. (9) occurs as a denominator in the equation for correcting the value of T each time step, and the method of integration fails when condition (9) occurs. Testing condition (9) is therefore quite simple.

The study of discretized integral equations like this one has only just begun. The sole instance I have found of such study barely touched on convolutions of the form of Eq. (1) and (2), and did not include the variable interval of integration [7].

Verification of the Results of Godfrey

The results given by Godfrey have been confirmed in each case in which they have been tested, with one exception which does not modify the important conclusions. Figure 5 shows the bifurcation diagram obtained by Godfrey as a function of α. His time step (normalized to the unperturbed transit time L/v_0) was roughly 1/50. His Poincaré section was chosen at the maximum value of $T(t)$ of each orbit. In order to make comparison of our results simpler, this same section was used in the present work even though it is not clear that it is a truly valid Poincaré section. (Choosing the maximum of T as the Poincaré section is not necessarily valid since the locus of all points which are maxima of T for different cycles is not necessarily a continuous or well-behaved curve in E-T space.)

Figure 6 shows the bifurcation diagram with a time step of 1/64. Although the attractors are very similar, there are significant differences, particularly in the smaller values of α. Successive

halving of the time step reveals that the diagrams generated by time steps of 1/256 and 1/512 are visually indistinguishable (see Fig. 7), but quite different from the diagram generated by Godfrey. While the strange attractor remains, as well as all other important results, it is necessary to conclude that the time step in Godfrey's work was not small enough to produce the accuracy necessary for generating the correct bifurcation diagram. In all the work which follows, a time step of 1/256 is used.

One casualty of the better convergence of the bifurcation diagram is the break Godfrey observed in a period-5 window (the attractor shifted suddenly from one position to another as α was varied continuously), since the entire period-5 window is an artifact of the incomplete convergence. (A window is a range of values of α over which the motion is regular, and the period number is the number of cycles about the center of the attractor the orbit makes before closing on itself.) An even more striking jump from one chaotic attractor to another was observed, however, in the bifurcation diagram for $C = 1000$ (C being the external capacitance), as will be discussed.

One of the most important results obtained by Godfrey is that the return map (a plot of each point of the Poincaré map versus its predecessor) appears to be one-dimensional, *i.e.*, a line with no thickness or structure. If the return map is truly one-dimensional, then it generates an irreversible sequence of points, *i.e.*, knowing everything about a point tells you what its successor will be, but its predecessor may be indeterminate. To verify this result, rather than use Godfrey's Poincaré section (which carries no guarantee of being a *continuous* section, *i.e.*, a smooth curve cutting across the trajectories in E and T space), a section is made at $T = 0$, $dT/dt < 0$. Also, consecutive values of E are plotted rather than values of T. Figure 7 is marked with the values of α for which return maps are shown in Figs. 8–12. Note that although the maps are not single-valued, they have no discernible structure within the line (except for one small spur on the most complex one). This implies that either the equations of motion are irreversible, or that the subdominant eigenvalue of perturbations about the chaotic orbit is *much* less than the dominant one. There is one clue that the second possibility may be the correct one in that very near the point at which the attractor ends (Fig. 12), the curve develops a spur on one of the bends in the lower right corner of the return map, which indicates that an infinitude of such spurs may exist for all values of α, but lie so close to the rest of the attractor that they cannot be seen. If this is the case, then the attractor is actually of fractional dimension (probably very close to dimension one), and the flow *could* then be completely time reversible.

The second, third, and fourth period-doubling bifurcations can be used to find an approximation to what one would expect to be Feigenbaum's number [3]. The values of α at these points are $\alpha_1 = 2.8581090 \pm .0000005$, $\alpha_2 = 2.8578912 \pm .0000002$, and $\alpha_3 = 2.8578442 \pm .0000001$, from which the value $(\alpha_1 - \alpha_2)/(\alpha_2 - \alpha_3) = 4.63 \pm .03$ which is in fairly good agreement with Feigenbaum's number 4.669.

An interesting, and to my knowledge unreported, phenomenon is noticeable in these bifurcation diagrams. A pattern of short vertical lines seems to follow a straight horizontal line from the last band-merging (at $\alpha = 2.85671\pi$) on. Fainter patterns can be seen starting from other band-mergings. This effect can be seen better in a blow-up of the region of the last band-merging (see Fig. 13). The effect is also observable in bifurcation diagrams derived from one-dimensional non-invertible maps (see [8]). This apparent structure is due to the presence of an unstable cycle. The system orbit is not likely to pass near this unstable cycle, but when it does, it tends to stay near it for a longer time, since both the approach and retreat are exponential (just as a ball rolling up and over a hill will spend most of its time near the top). Thus, since only a limited number of orbits are completed for each value of α, some values of α will show no points near the unstable cycle, and others will show many. On the average, the density of points is neither enhanced nor depleted at these unstable cycles.

Godfrey also commented on the destruction of the strange attractor resulting from the collision of the attractor with an unstable equilibrium, a situation called a crisis [9]. Discussion of this phenomenon will be deferred until the results for finite values of the external capacitor have been described, since they add much to the evidence.

Strange Attractor with an External Capacitor

Before examining the behavior of the strange attractor as the capacitance is varied, it is important to examine the linear and equilibrium characteristics of this region as a function of the capacitance. The real part of the growth rate is shown as a function of α for several values of the capacitance in Fig. 14. Note that for infinite capacitance, the growth rate is zero for $\alpha = 2\pi$, and negative for a short region of α just less than 3π. With the introduction of a large external capacitance, the growth rate at 2π becomes negative (the transition from negative to positive, at α slightly larger than 2π, also becomes a Hopf bifurcation), and the growth rates near $\alpha = 3\pi$ become *less* negative. This trend continues until the external capacitance $C = 8$, at which point the growth

rate at $\alpha = 3\pi$ becomes exactly zero (as can be shown from the dispersion relation). At $C = 8$, the growth rate is entirely non-negative near $\alpha = 3\pi$. The growth rate for $\alpha = 3\pi$ peaks at $C = 8$, so for $C < 8$, it once again becomes negative near $\alpha = 3\pi$ (see Fig. 15). As C becomes smaller, the growth rate is positive for a narrower and narrower range of α, until at roughly $C = 4$, the system is linearly stable for all $2\pi < \alpha < 3\pi$.

The unstable equilibrium, which is responsible for the crisis which terminates the strange attractor, is a sensitive function of C. Figure 16 shows the value of E_0 at the unstable equilibrium versus α for several values of C. The equilibrium ceases to exist physically for $E_0 < -\alpha$, but is still present mathematically, and may still have an effect on the trajectory of the solution. The equilibrium values of T tend to increase as C is decreased.

Now let us examine how the attractor changes with the external capacitance. First I will simply describe the changes, then I will offer some interpretations.

The shape of the bifurcation diagram changes rapidly with even rather large values of C. Figure 17 shows the bifurcation diagram for $C = 1000$, and already the shape is much altered (compare Fig. 7). This bifurcation diagram shows an interesting jump in the attractor at $\alpha = 2.8515\pi$. Both attractors appear to be chaotic, but the solution jumps suddenly from one to the other.

Figures 18 and 19 show the bifurcation diagrams for $C = 100$ and $C = 20$. One obvious trend is that as the capacitance is decreased, the amplitude at which the crisis occurs increases. Between $C = 11$ and $C = 10$, the strange attractor rapidly disappears. Figures 20–22 show the bifurcation diagrams for $C = 11$, $C = 10.7$, and $C = 10.4$. The bifurcation diagram for $C = 10$ shows no bifurcations (aside from the initial Hopf bifurcation leading to the non-uniform solution).

While the strange attractor has vanished, the behavior for values of C less than 10 is interesting. Between $C = 9$ and roughly $C = 6$, the stable limit cycle seems to cease to exist. In fact, it probably is just stable over a very narrow range of values of α, with the possible exception of $C = 8$, which has no Hopf bifurcation (the growth rate is not negative, and a double root exists at $\alpha = 3\pi$.

In the meantime, the solution for smaller α (the point of zero linear growth near $\alpha = 2\pi$ is a Hopf bifurcation for all finite values of C), becomes stable over a wider and wider range of α as C is decreased. At no time, however, does this other stable limit cycle show signs of bifurcations or chaotic behavior. At roughly $C = 5$, this limit cycle meets the limit cycle originating at higher α, forming one continuous limit cycle as a function of α (see Fig. 23). At roughly $C = 4$, the most

unstable growth rate becomes zero, and only the uniform equilibrium is stable for all α between 2π and 3π.

Returning now to the strange attractor, Fig. 24 shows the orbit in E and T of the solution for $C = 11$ near the crisis ($\alpha = 2.758\pi$). The unstable equilibrium is marked as a large dot (not to be confused with the large blob at $E = 0$, $T = 1$). Just as in the $C = \infty$ case the unstable equilibrium is clearly disturbing the attractor to the point at which it may create a hole in the attractor basin.

The shape of this orbit is rather complex, and it can be seen that one orbit does not even cross $T = 1$, making the chosen Poisson section of dubious value. For the sake of consistency, though, the return map will still be plotted at $T = 1$.

Now some general comments comparing the crisis observed in the Pierce Diode and the crises studied by Grebogi, Ott, and Yorke [9] are in order. Grebogi *et al.* studied non-invertible maps with one variable whose return map was known as a function of some parameter. It is possible that the Pierce diode attractor can be reduced to such a map, and it can almost certainly be reduced to a similar problem which is a non-invertible, one-dimensional map [10]. If this can be done, the E is almost certainly not the best variable to use. A change of variable is in order, but the proper variable, one which contains all the relevant information and no extraneous information, has not been found. This variable, if it exists, would produce a simple, roughly parabolic return map as has been studied by Ott and Grebogi, and it is to be hoped that its value at the uniform equilibrium would exactly coincide with the crisis.

In the cases studied by Ott and Grebogi, the strange attractor ceased to exist only when the unstable cycle exactly contacted the attractor. It is this predictive power which makes the concept so powerful. Here, though, only the existence of the unstable equilibrium is known, and the destruction of the attractor, while clearly associated with the unstable equilibrium, cannot be predicted with any accuracy. Plainly there is more of importance to the system at any given time than E and T at that time, since these values pass over and around the equilibrium values without creating any large disruption. Only when the value of E remains near the equilibrium value for a longer period of time does the equilibrium seem to greatly influence the solution.

An interesting question is whether the unstable equilibrium is necessary for the *formation* of the strange attractor. The lack of any strange attractor in the region just above $\alpha = 2\pi$ for any value of C is suggestive of this, since the unstable equilibrium for this region is far away from the solution (in fact, the unstable equilibrium is in the unphysical $E < -\alpha$ region).

Also suggestive is the character of the orbits. The orbits seem regular, and seldom cross just before they encounter the unstable equilibrium ($T < 1$ and $E < 0$), but as they pass near it, they diverge, and immediately afterward, they reconverge, crossing in the process. This seems to indicate that the unstable equilibrium is responsible for the exponential divergence of neighboring orbits required for a strange attractor, and that without it (if such an idea is meaningful) the orbits would quickly converge to a steady (oscillatory) state.

Summary

The work of Godfrey on the Pierce diode strange attractor has been verified (with one minor correction). The strange attractor was found where expected, and followed the prediction of Feigenbaum regarding the cascade of bifurcations leading to chaos. Only the detailed structure was found to differ from Godfrey's result, this being attributed to insufficiently small time steps in Godfrey's numerical integration of the equations.

The strange attractor was studied as an external capacitance was introduced and varied, and the results were discussed. In particular, it was suggested, on the basis of circumstantial evidence, that the unstable equilibrium is necessary not only for the destruction of the attractor (in a crisis), but for the existence of the strange attractor.

Acknowledgments

I gratefully acknowledge the advice and assistance of Dr. B. B. Godfrey and Prof. M. A. Lieberman, and the support of Prof. C. K. Birdsall. This work was supported by Dept. of Energy contract number DE-AT03-76ET53064 and Office of Naval Research contract number N00014-85-K-0809.

References

[1] J. R. Pierce, *J. Appl. Phys.* **15**, 721 (1944)

[2] B. B. Godfrey, *Phys. Fluids* **30**, 1553 (1987)

[3] M. J. Feigenbaum, *J. Stat. Phys.* **19**, 25 (1978)

[4] S. Kuhn and M. Hörhager, *J. Appl. Phys.* 60, 1952 (1986)

[5] Wm. S. Lawson, UCB/ERL memo M87/51

[6] Wm. S. Lawson, UCB/ERL memo M87/52

[7] A. Fulinski and A. S. Kleczkowski, *Phys. Scr.* **35**, 119 (1987)

[8] A. J. Lichtenberg and M. A. Lieberman, *Regular and Stochastic Motion* (Springer-Verlag, New York, 1983), p. 418

[9] C. Grebogi, E. Ott, and J. A. Yorke, *Physica D* **7**, 181 (1983)

[10] E. Ott, *Rev. M. Phys.* **53**, 655 (1981)

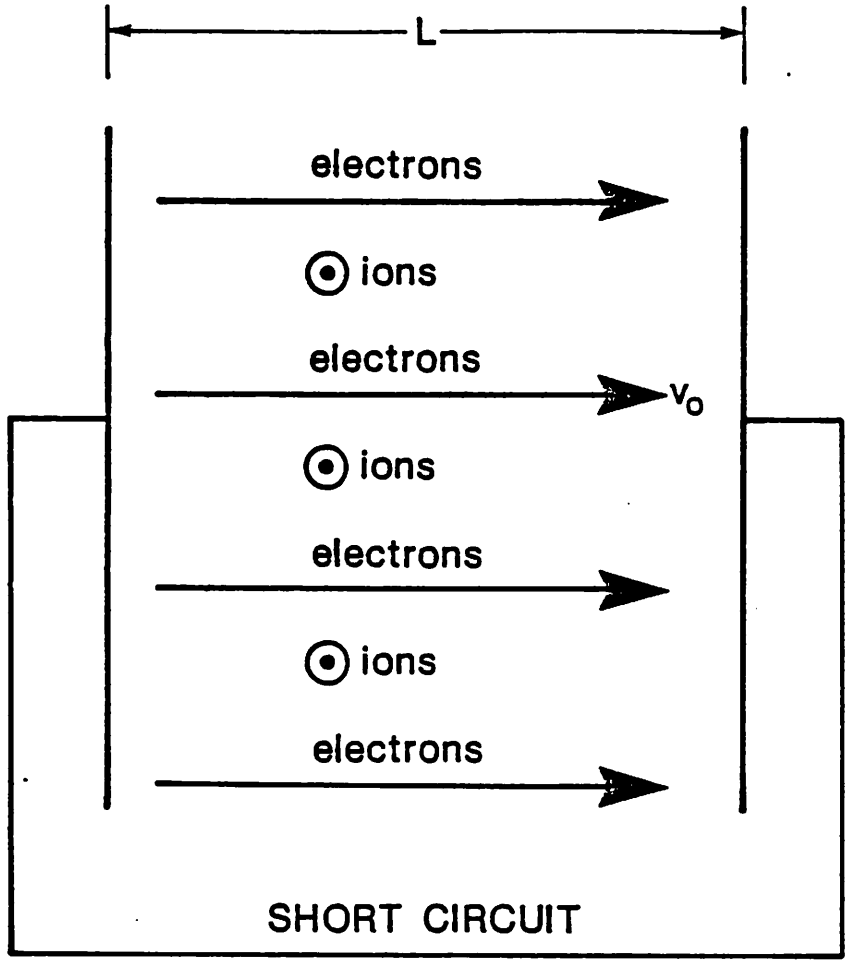

Fig. 1. Ordinary Pierce Diode model

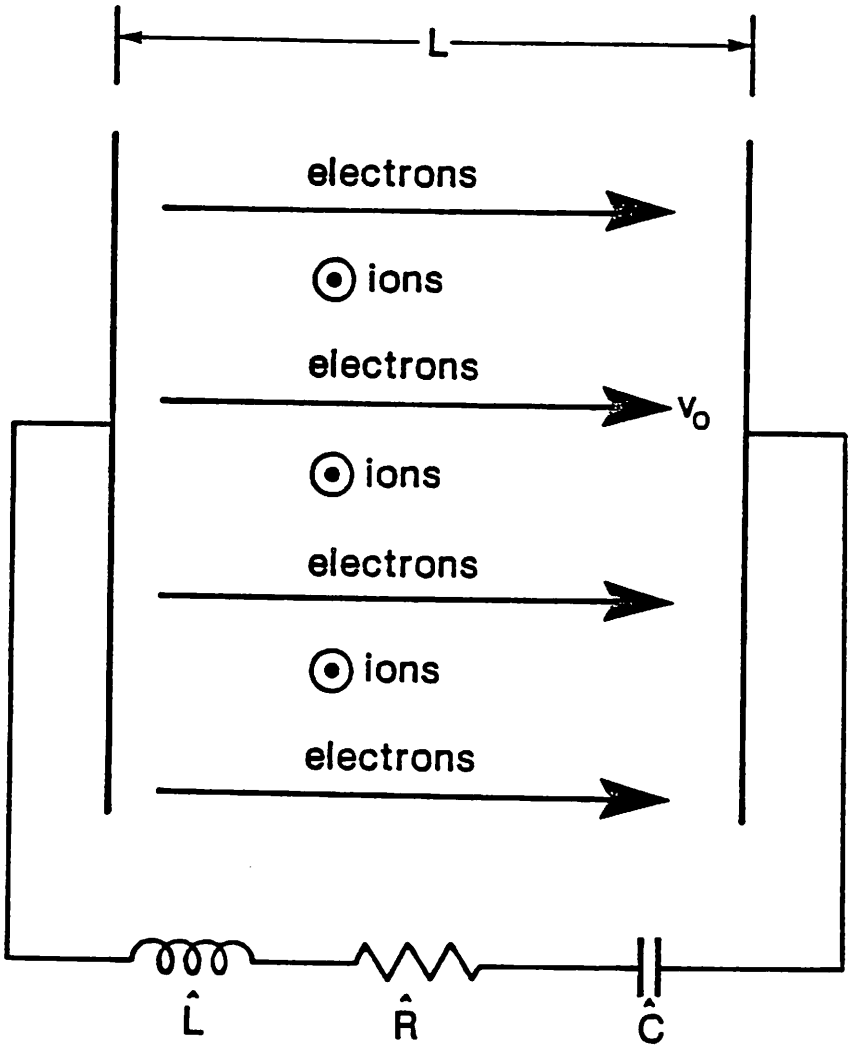

Fig. 2. Extended Pierce Diode model

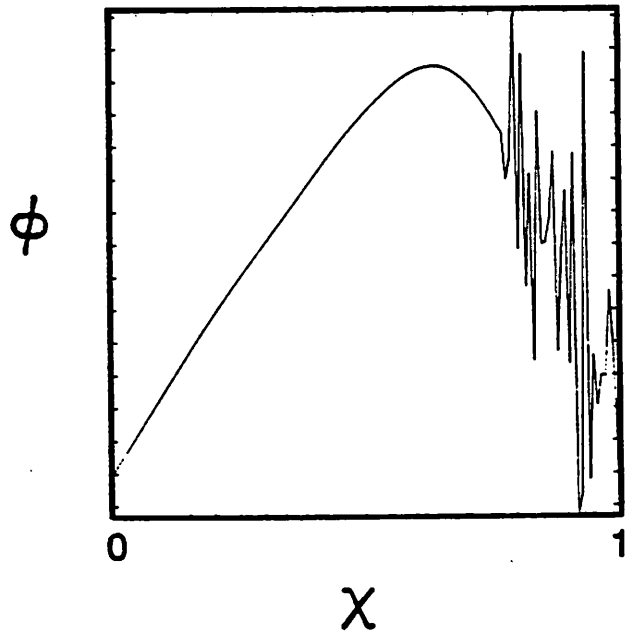

Fig. 3. Pierce Diode simulation run before initially loaded particles have left system

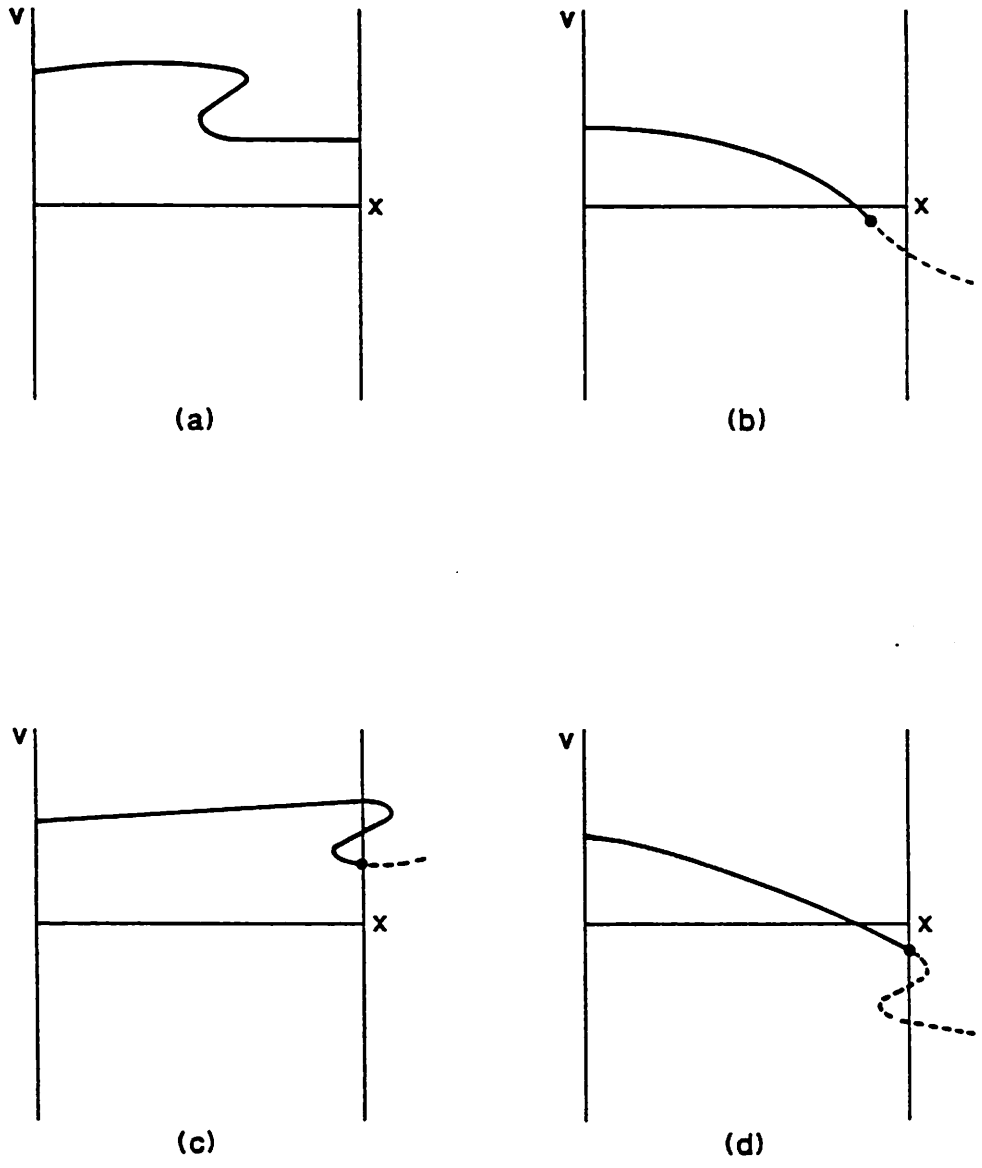

Fig. 4. Situations which limit the physical and mathematical validity of the solution. In (a), the velocity is not a single-valued function of position, in (b), particles which have left the model return; in (c) and (d), the transit time T ceases to exist.

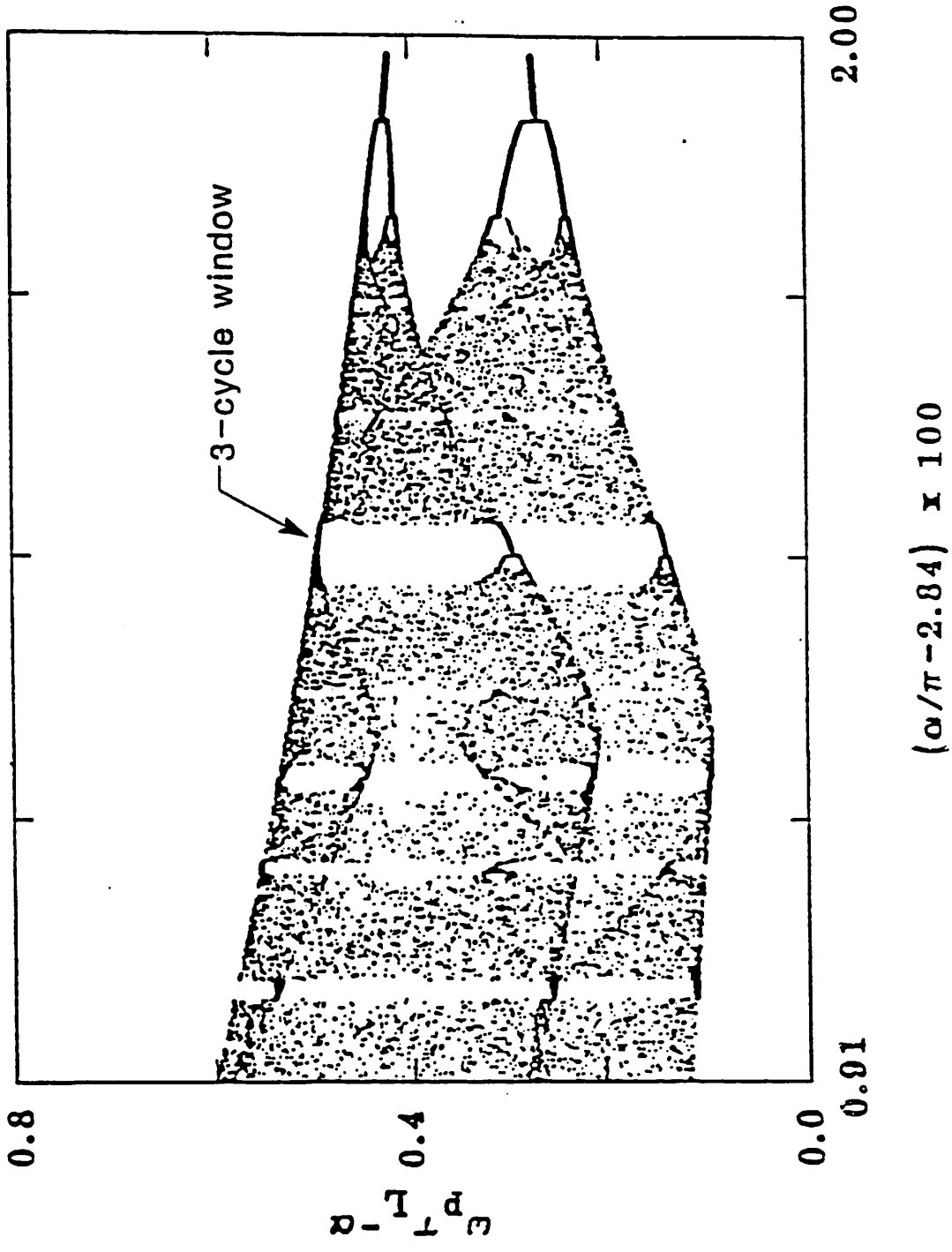

Fig. 5. Bifurcation diagram obtained by Godfrey. A 3-cycle window is indicated by the arrow. The first bifurcation is off the right side of the plot, but the second bifurcation is visible as a pair of Y's.

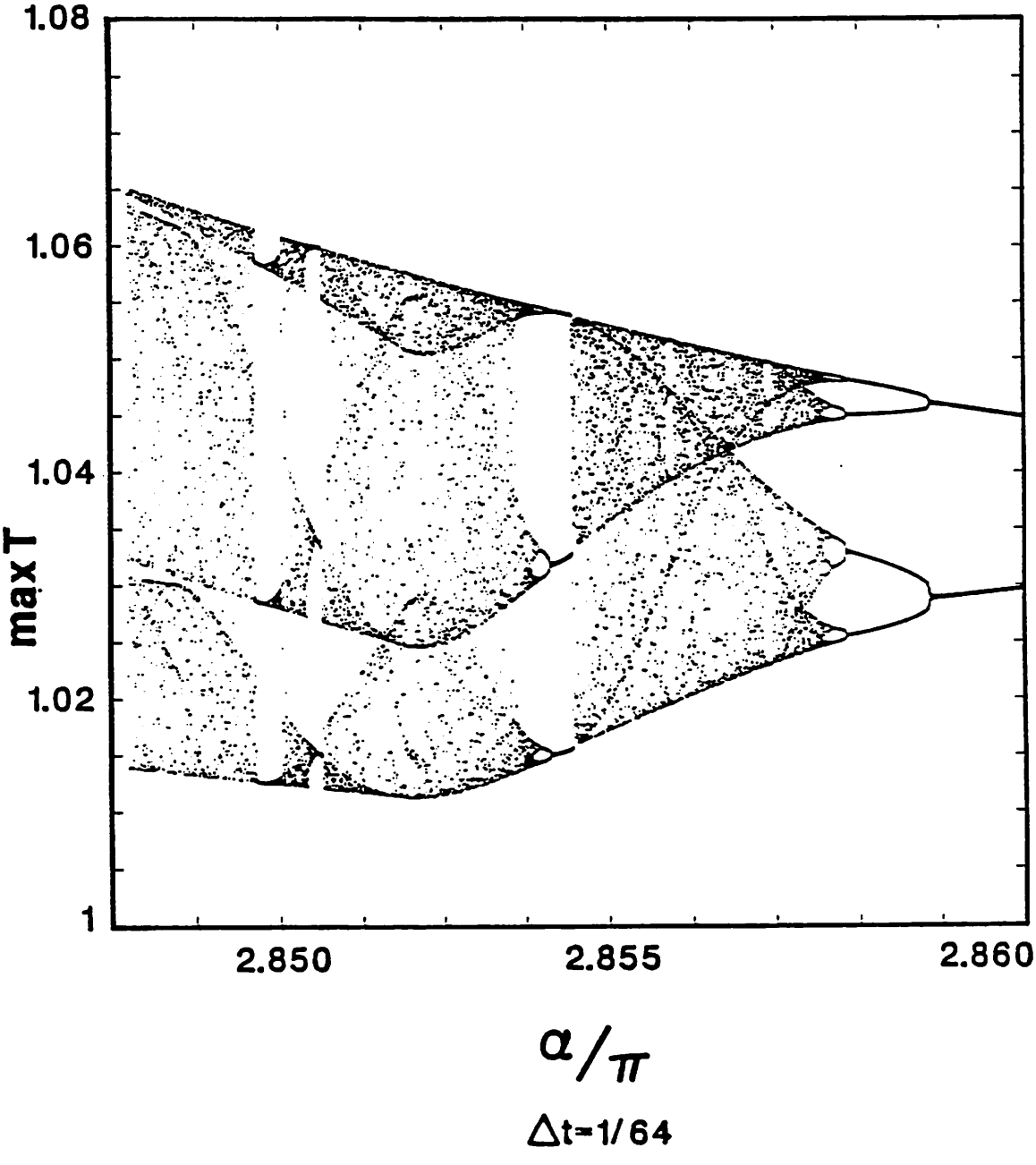

Fig. 6. Bifurcation diagram for $\Delta t = 1/64$ (not yet converged)

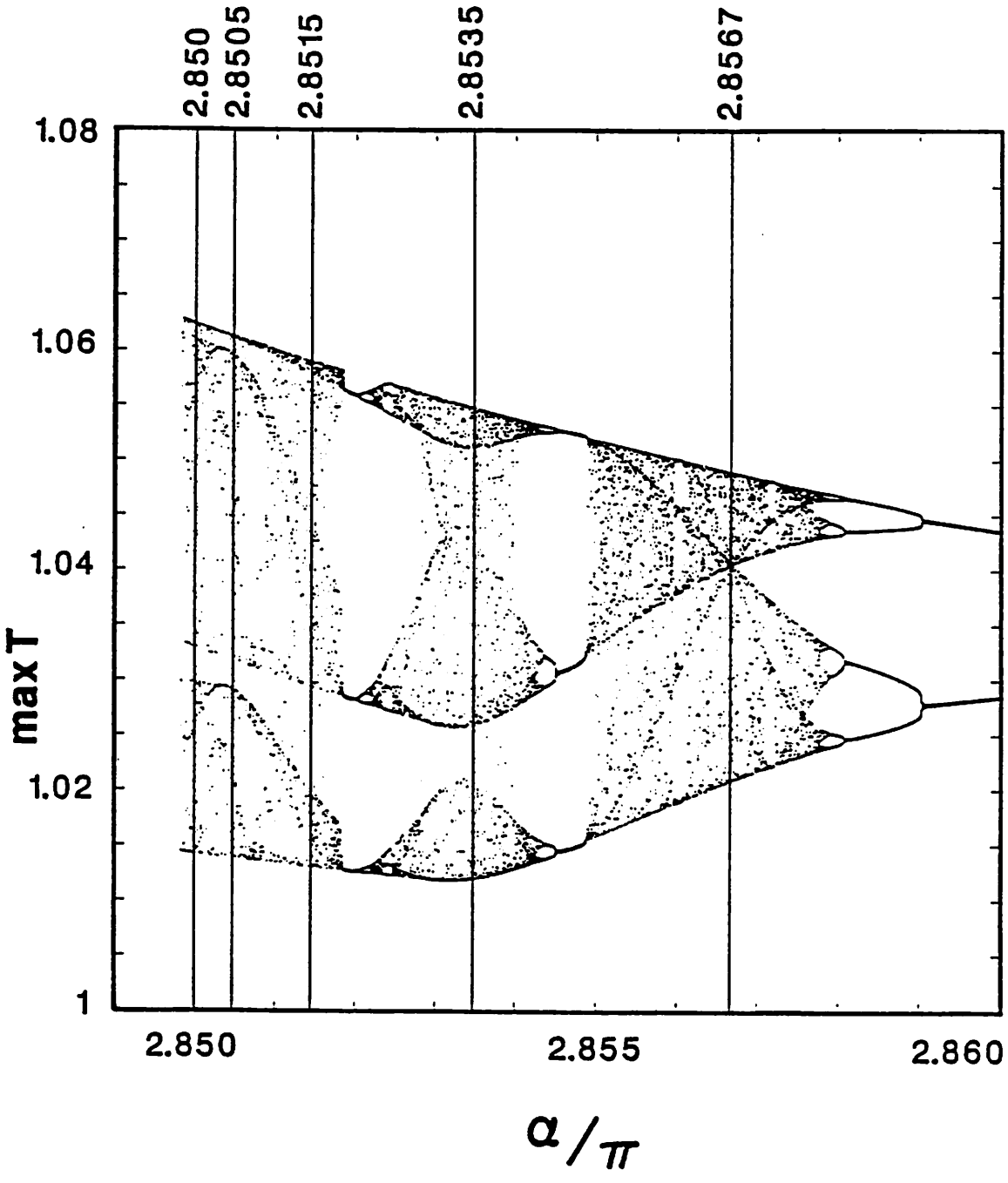

Fig. 7. Bifurcation diagram for $\Delta t = 1/256$ (indistinguishable from diagram for $\Delta t = 1/512$). The vertical lines mark the values of α at which return maps will be plotted.

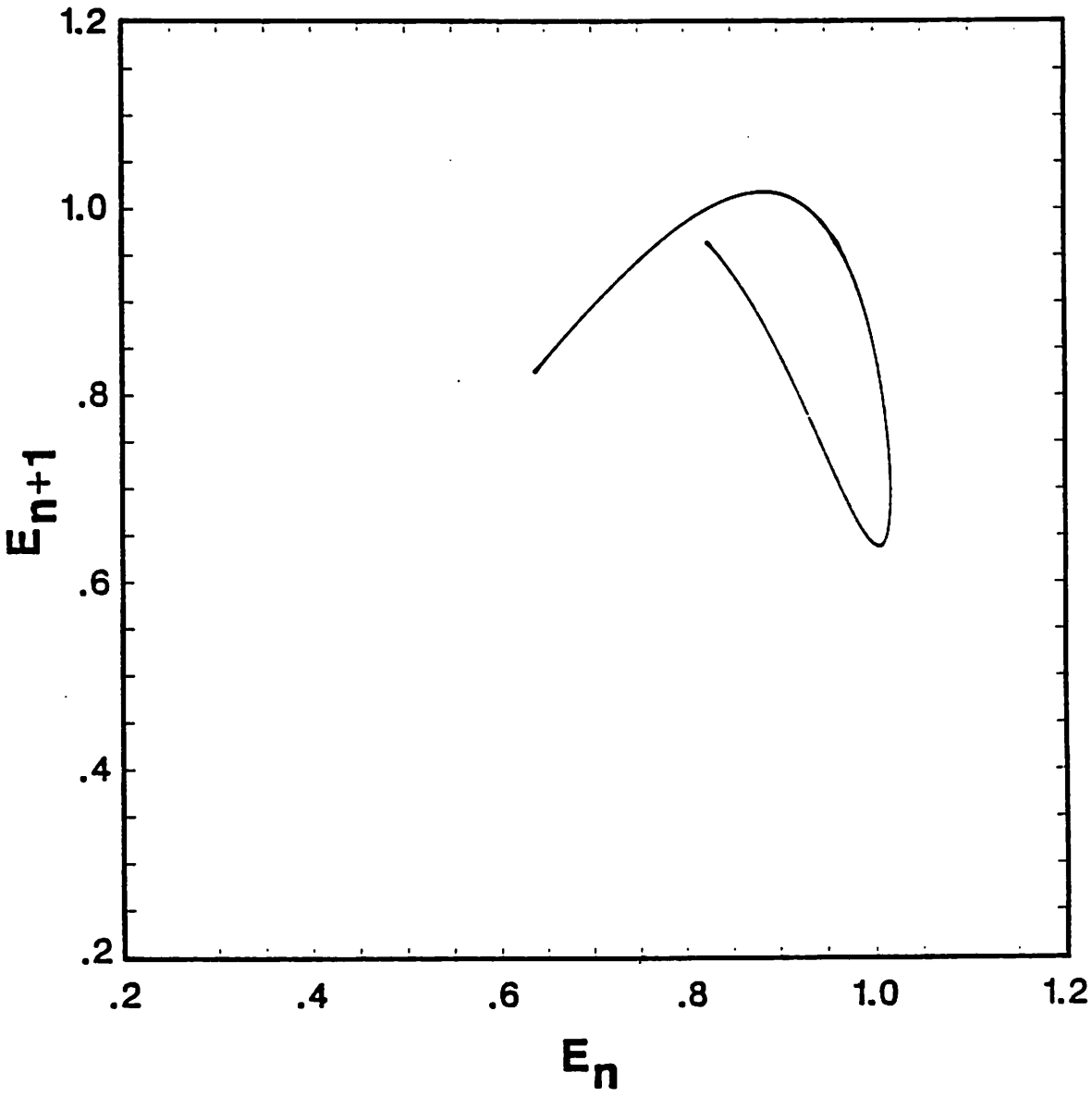

Fig. 8. Return map for $\alpha = 2.8567\pi$

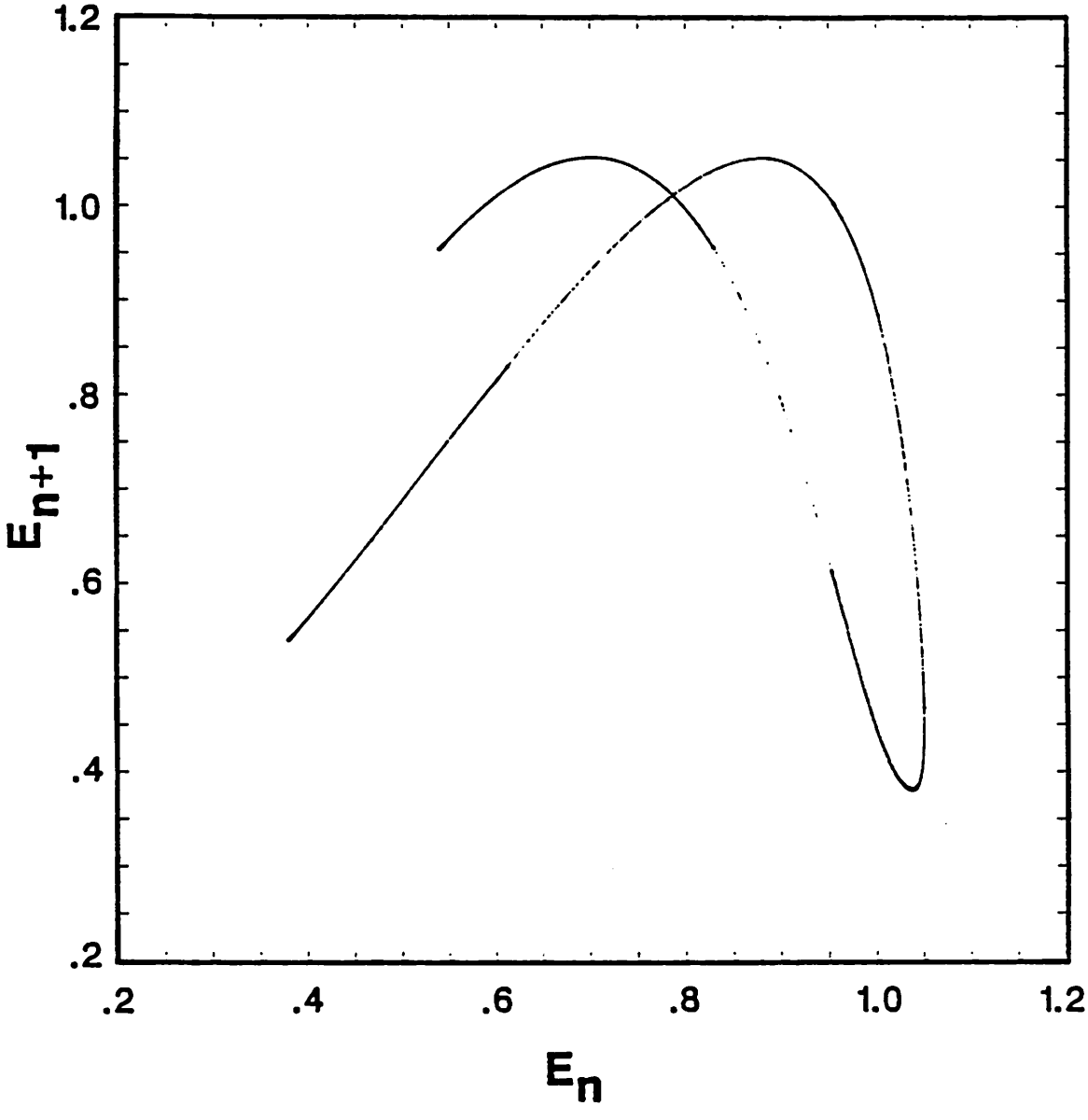

Fig. 9. Return map for $\alpha = 2.8535\pi$

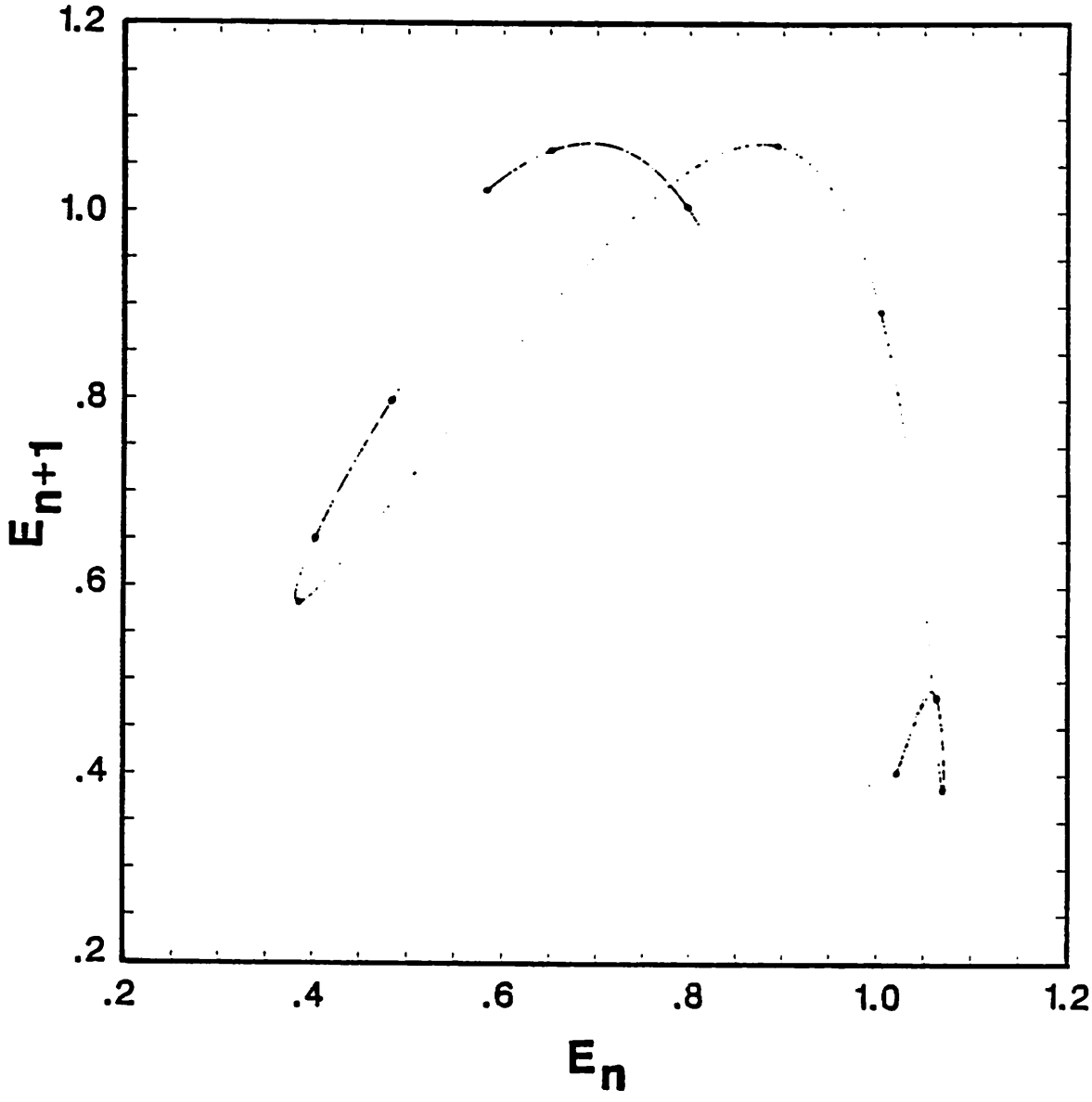

Fig. 10. Return map for $\alpha = 2.8515\pi$. Note the dots indicating a possible stable 11-cycle.

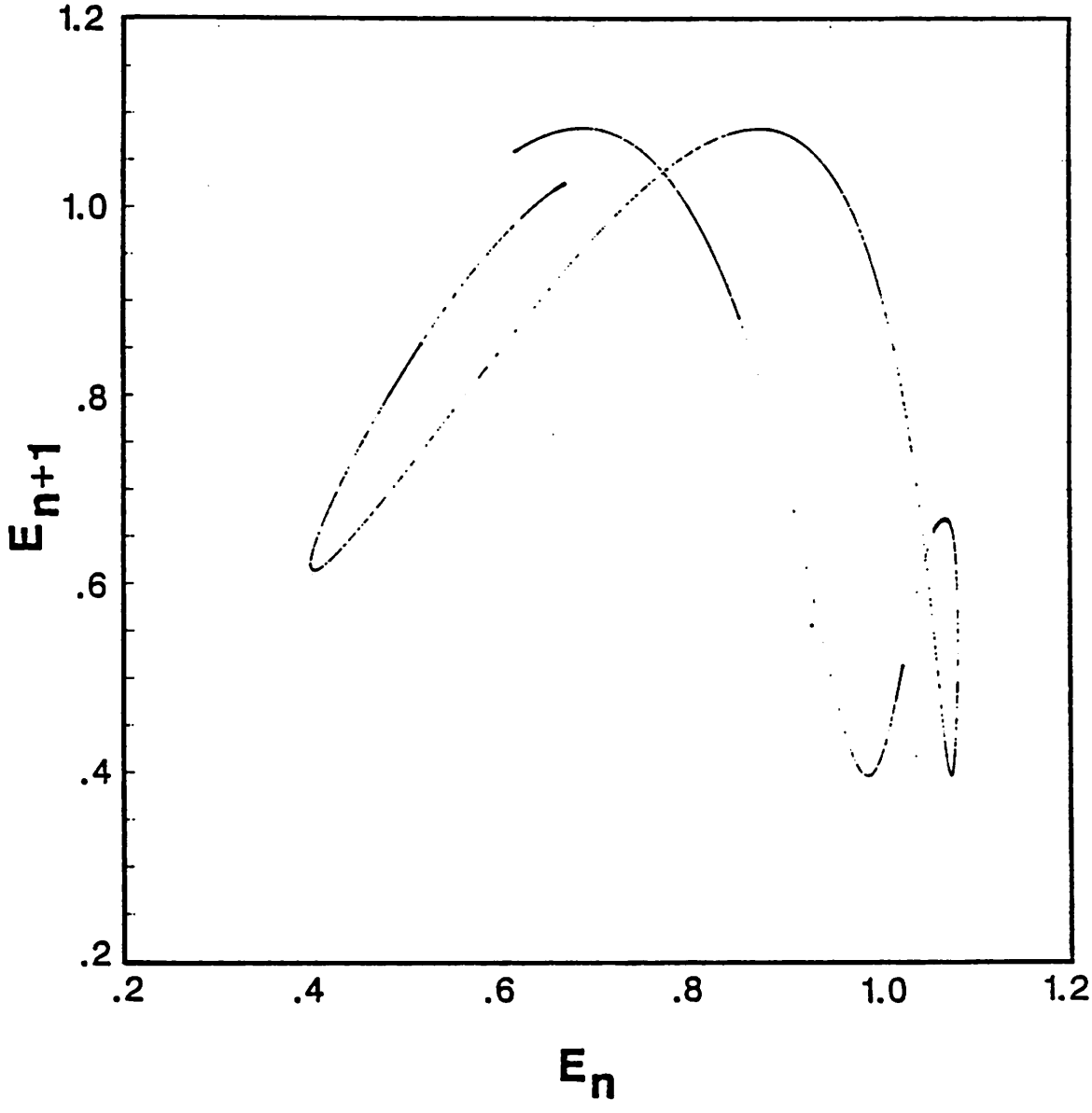

Fig. 11. Return map for $\alpha = 2.8505\pi$

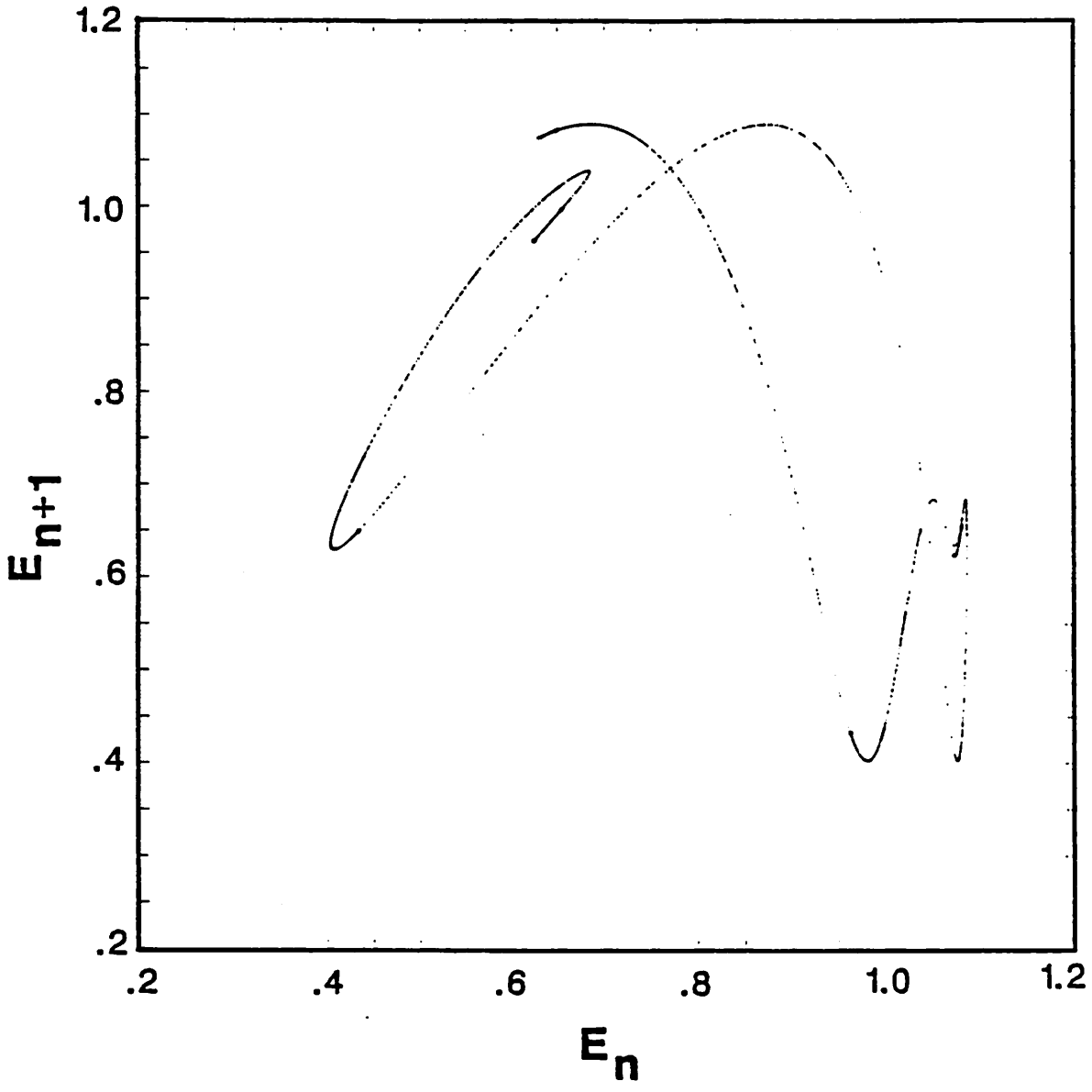

Fig. 12. Return map for $\alpha = 2.8500\pi$. Note the spur in lower right-hand section of curve, indicating that the curve may have much unresolved structure.

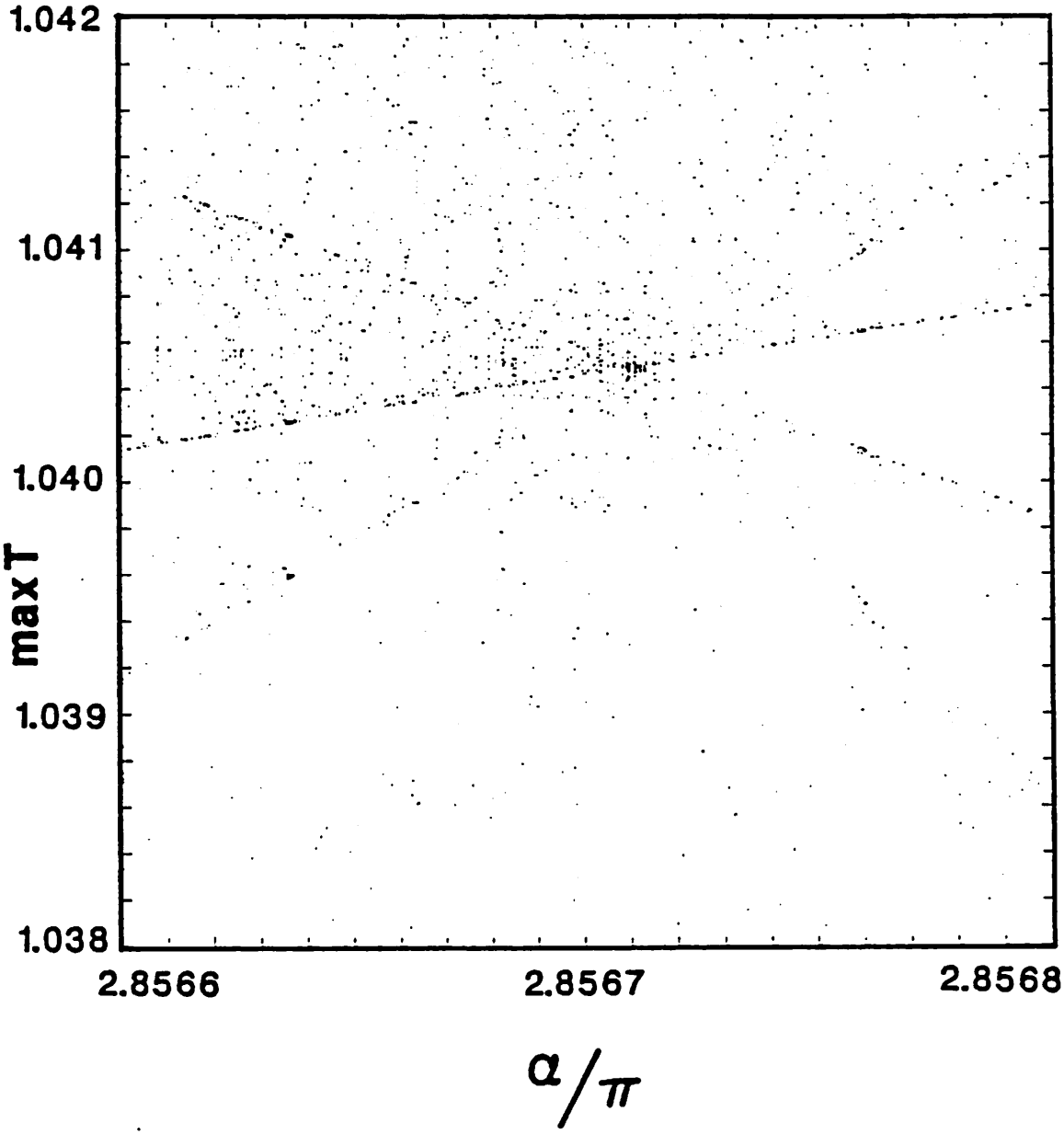

Fig. 13. Blow-up of bifurcation diagram near last band-merging, showing the effect of the unstable equilibrium

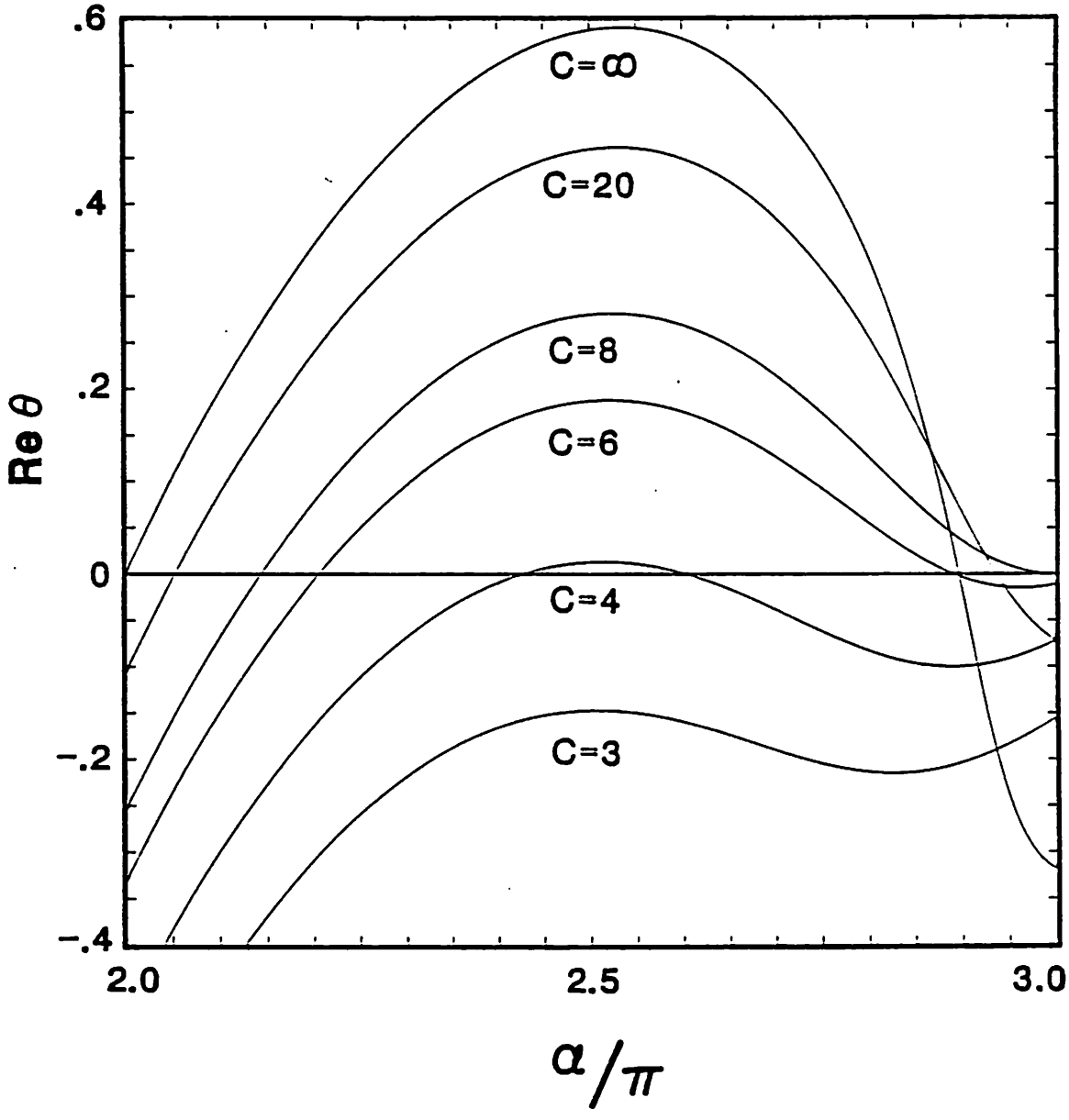

Fig. 14. Real part of the linear growth rate from the uniform equilibrium between $\alpha = 2\pi$ and $\alpha = 3\pi$ for several values of the external capacitance C

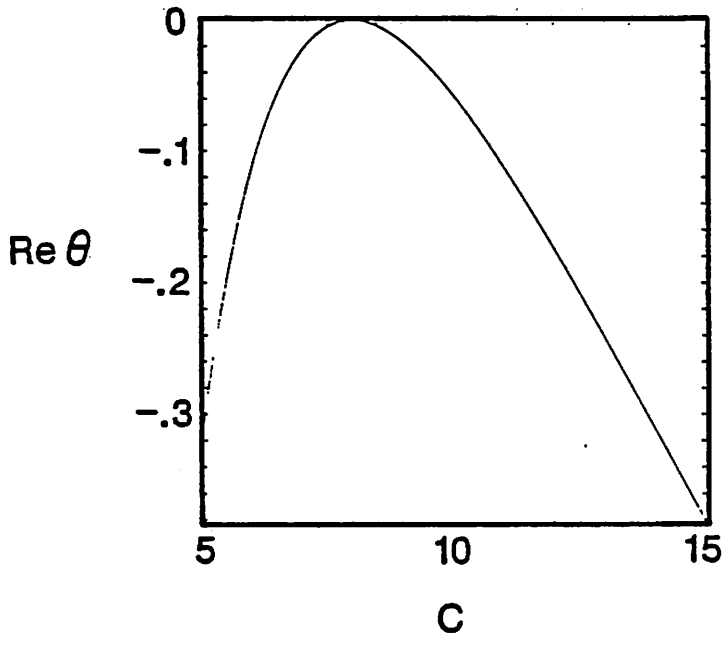

Fig. 15. Real part of the linear growth rate at $\alpha = 3\pi$ as a function of the external capacitance C

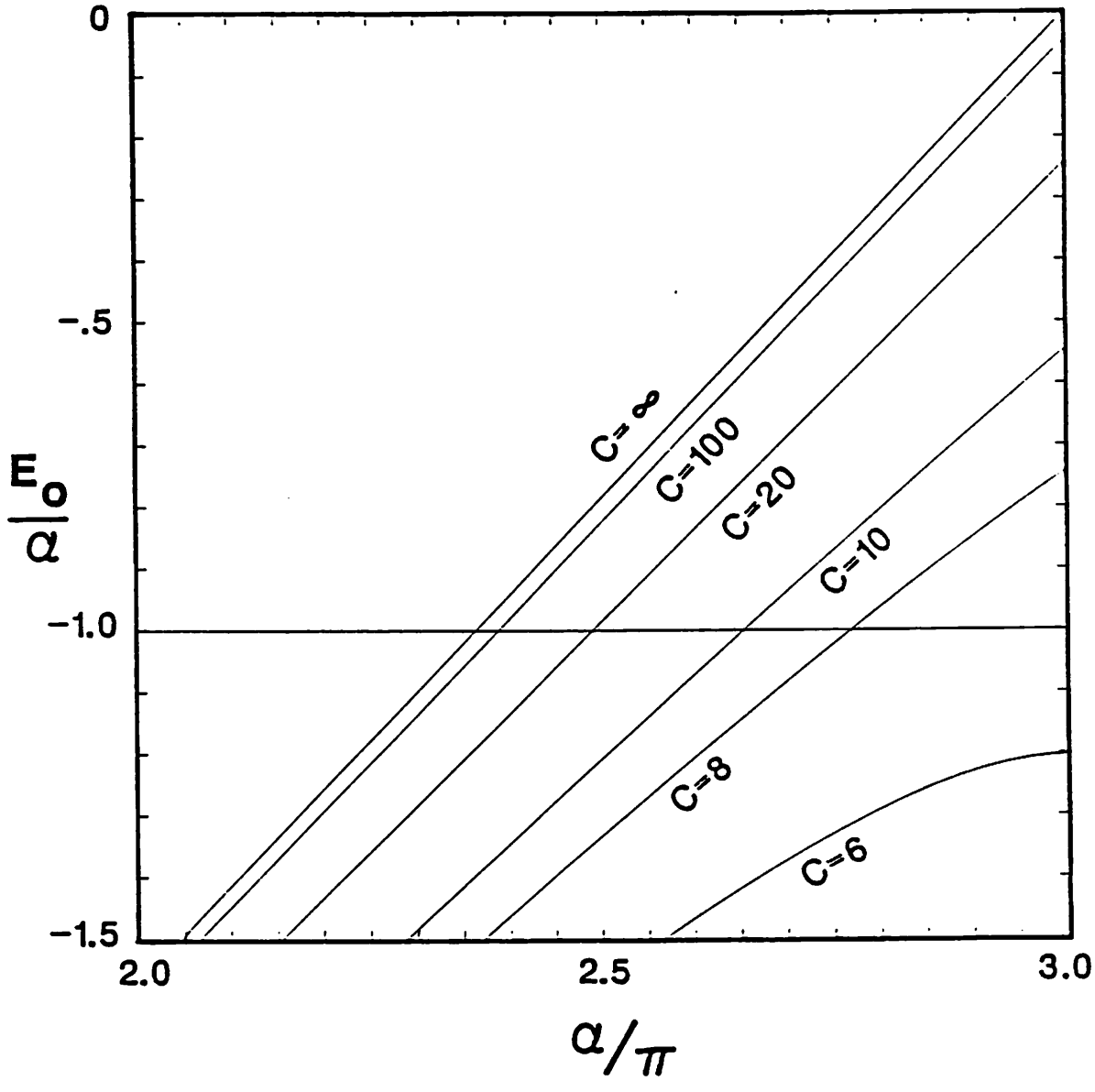

Fig. 16. Values of E_0 at the unstable equilibrium as a function of α for several values of the external capacitance C

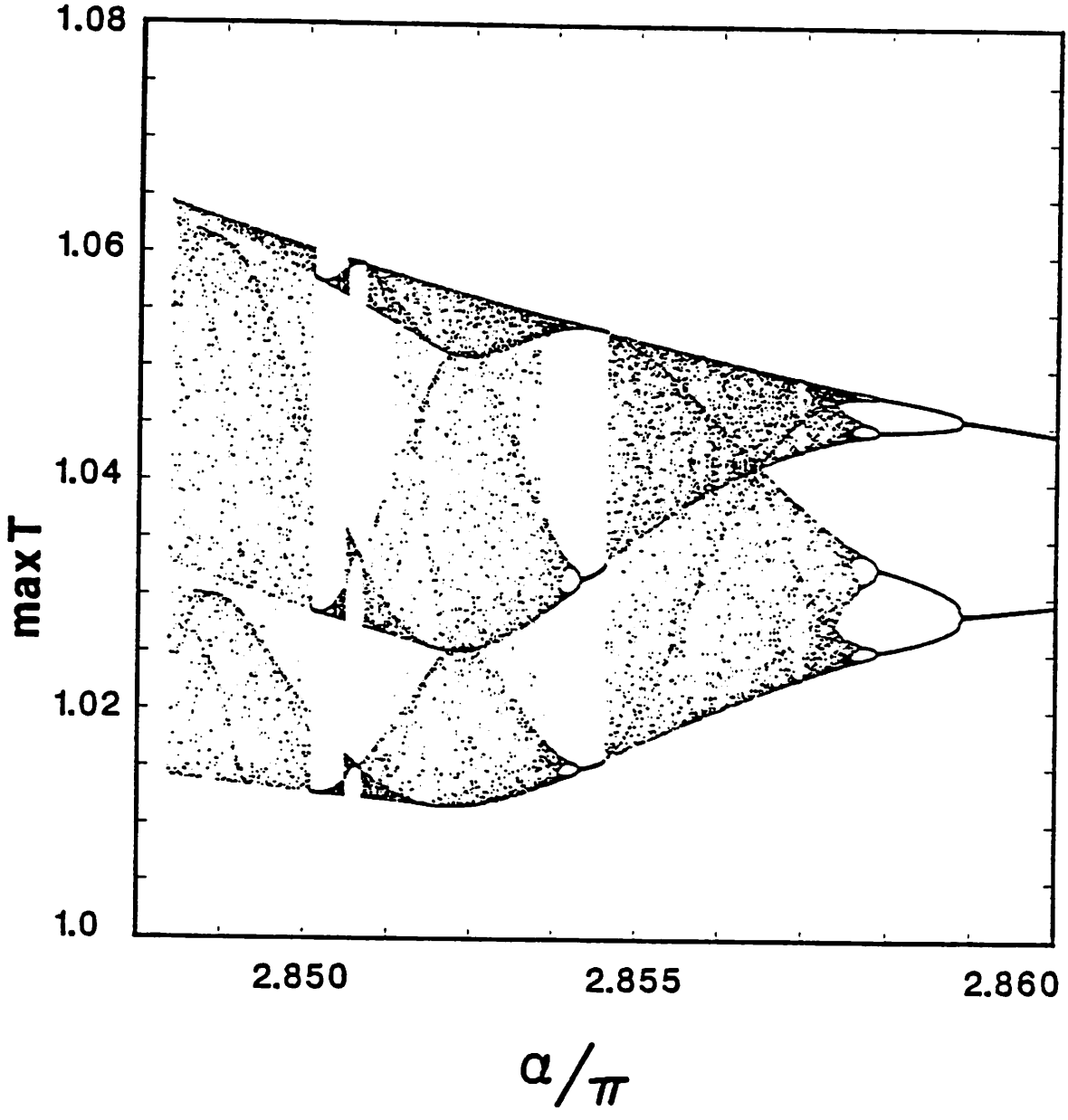

Fig. 17. Bifurcation diagram for $C = 1000$

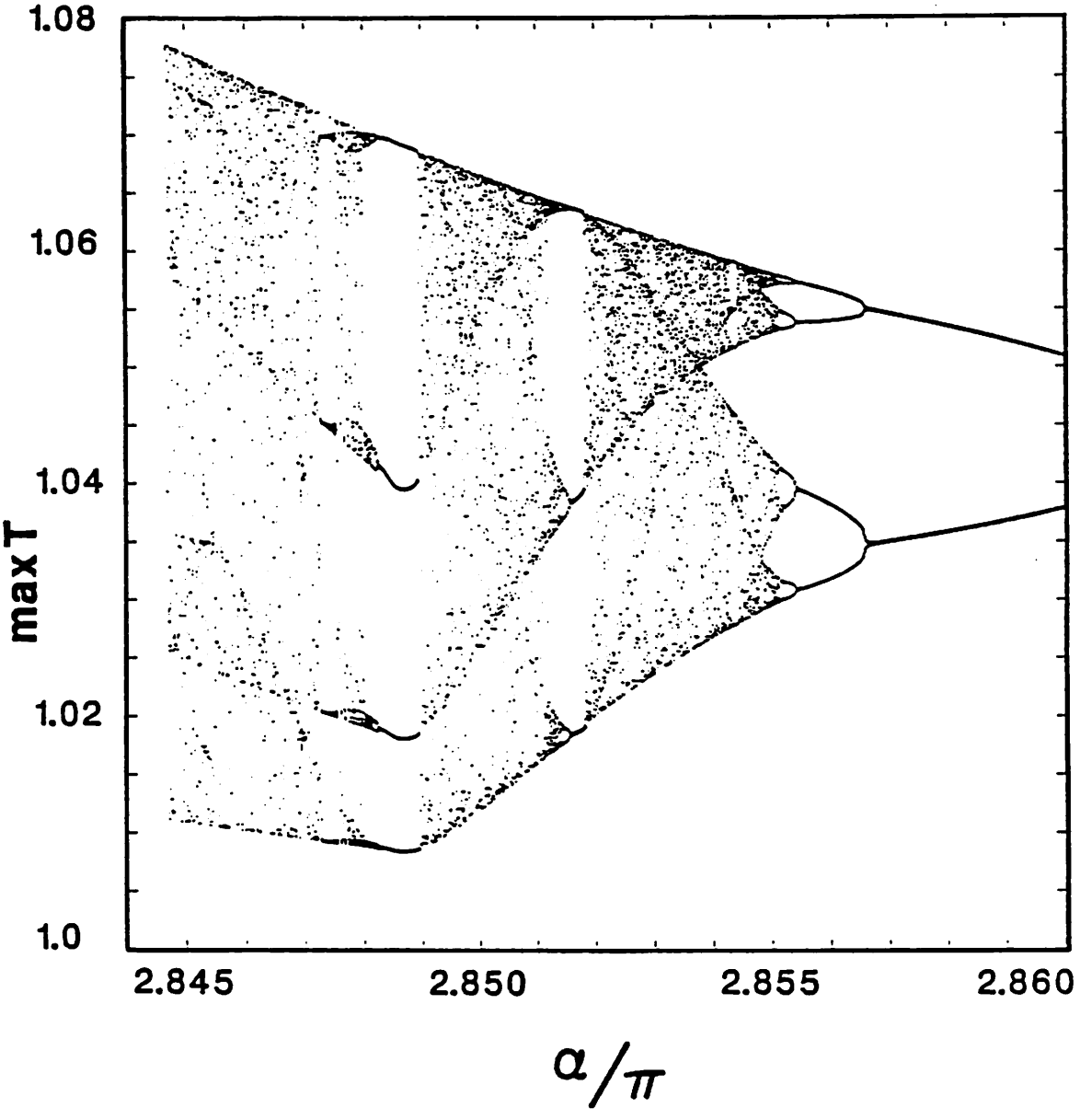

Fig. 18. Bifurcation diagram for $C = 100$

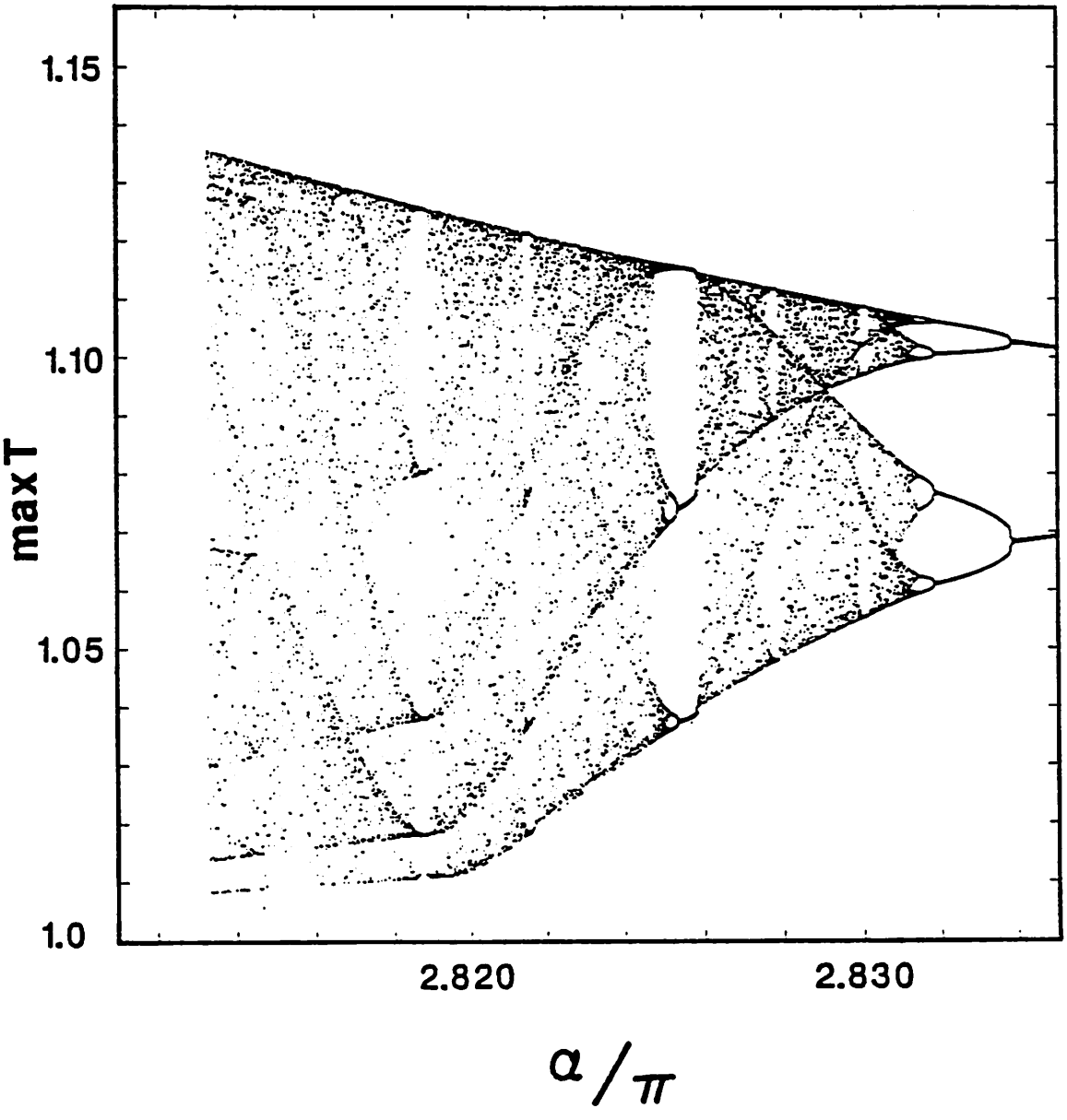

Fig. 19. Bifurcation diagram for $C = 20$

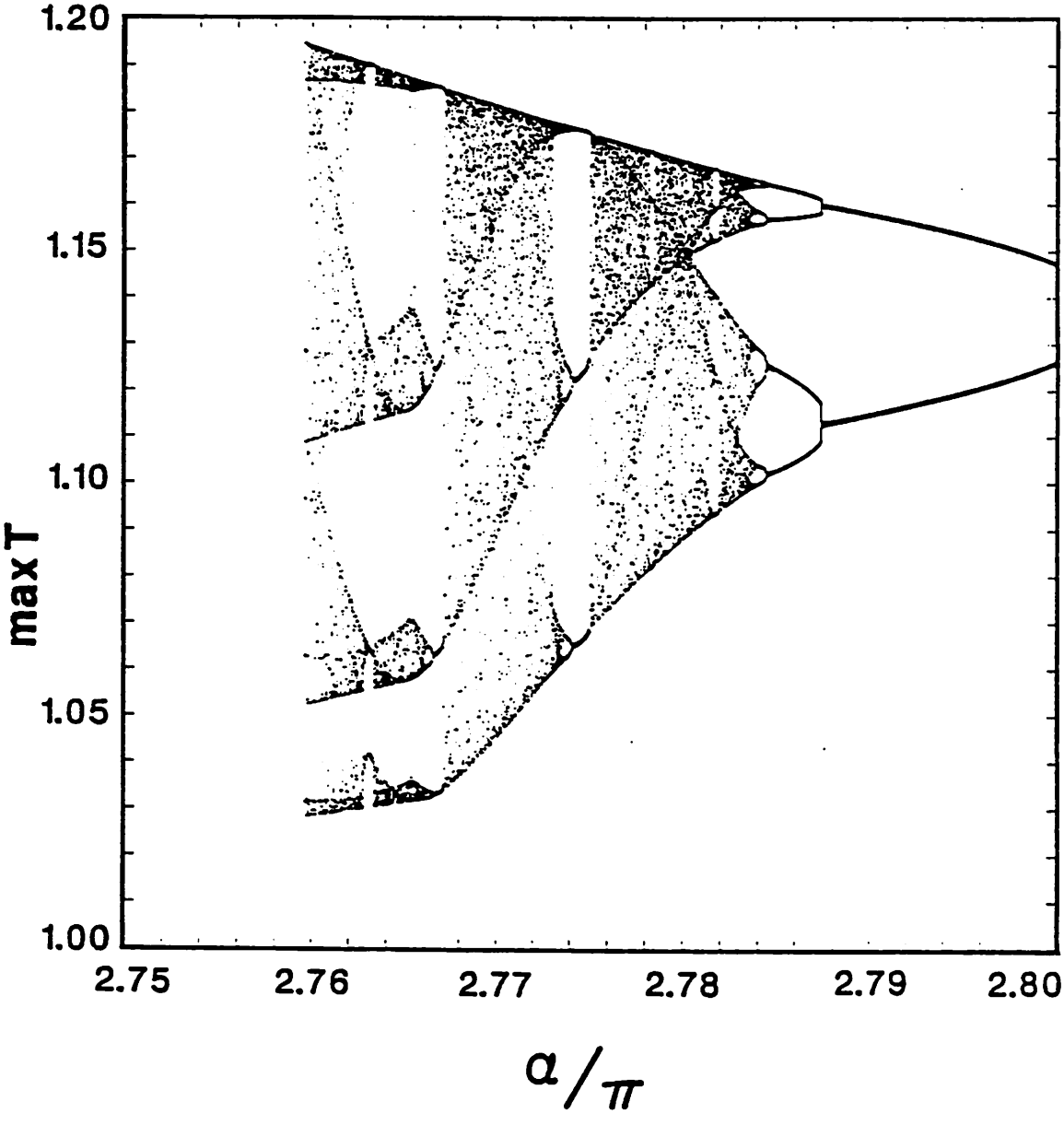

Fig. 20. Bifurcation diagram for $C = 11$

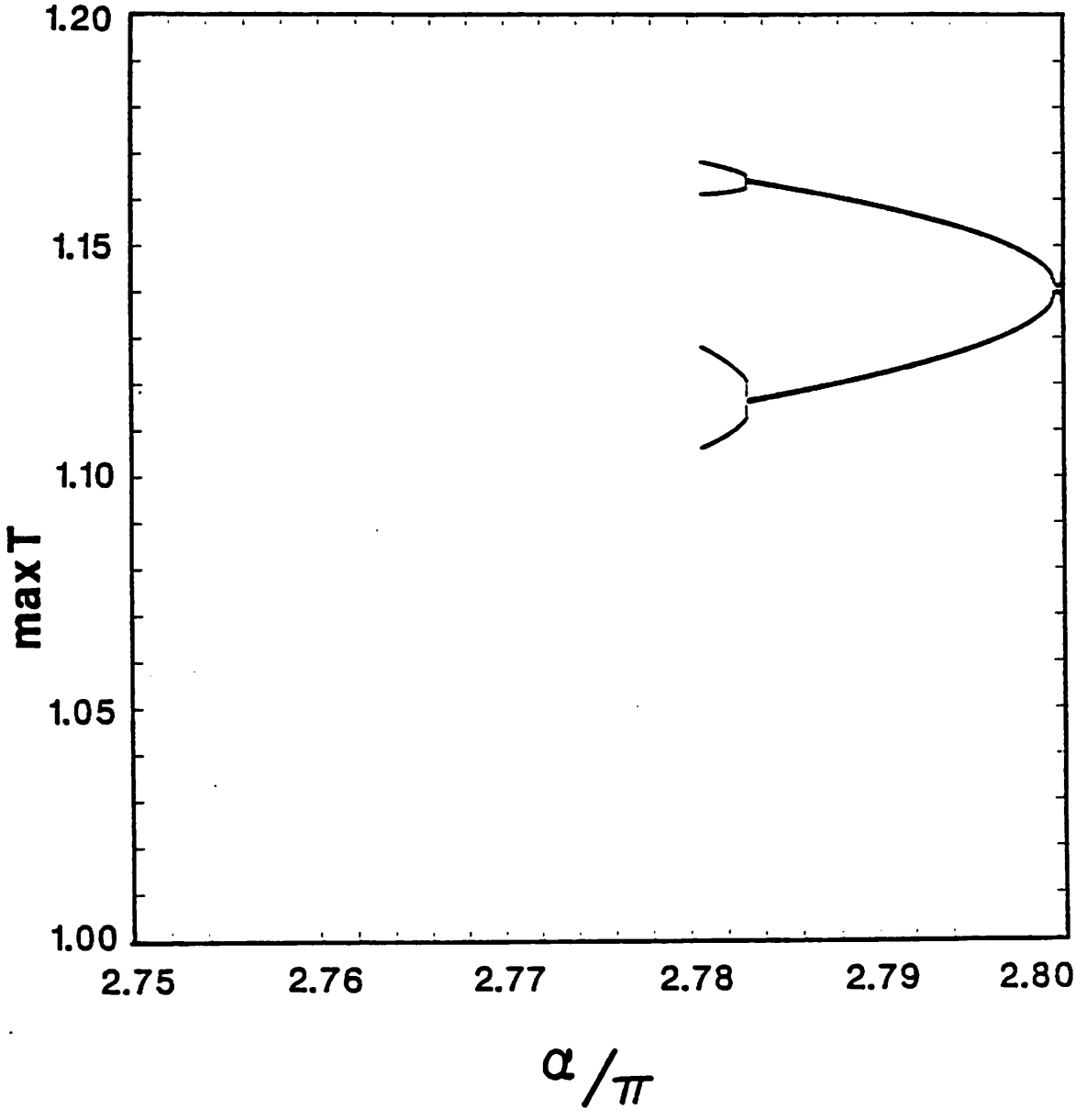

Fig. 21. Bifurcation diagram for $C = 10.7$

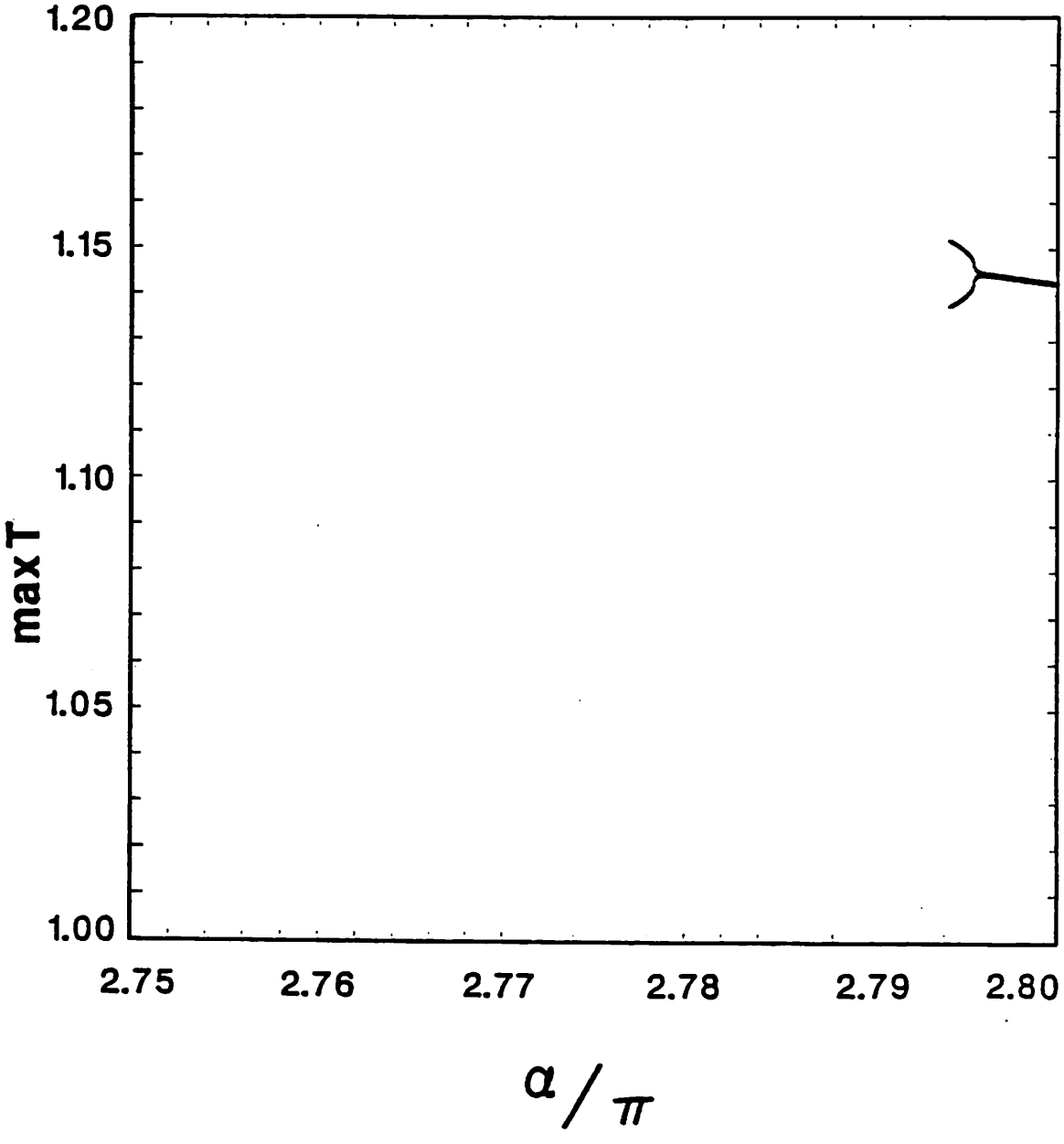

Fig. 22. Bifurcation diagram for $C = 10.4$

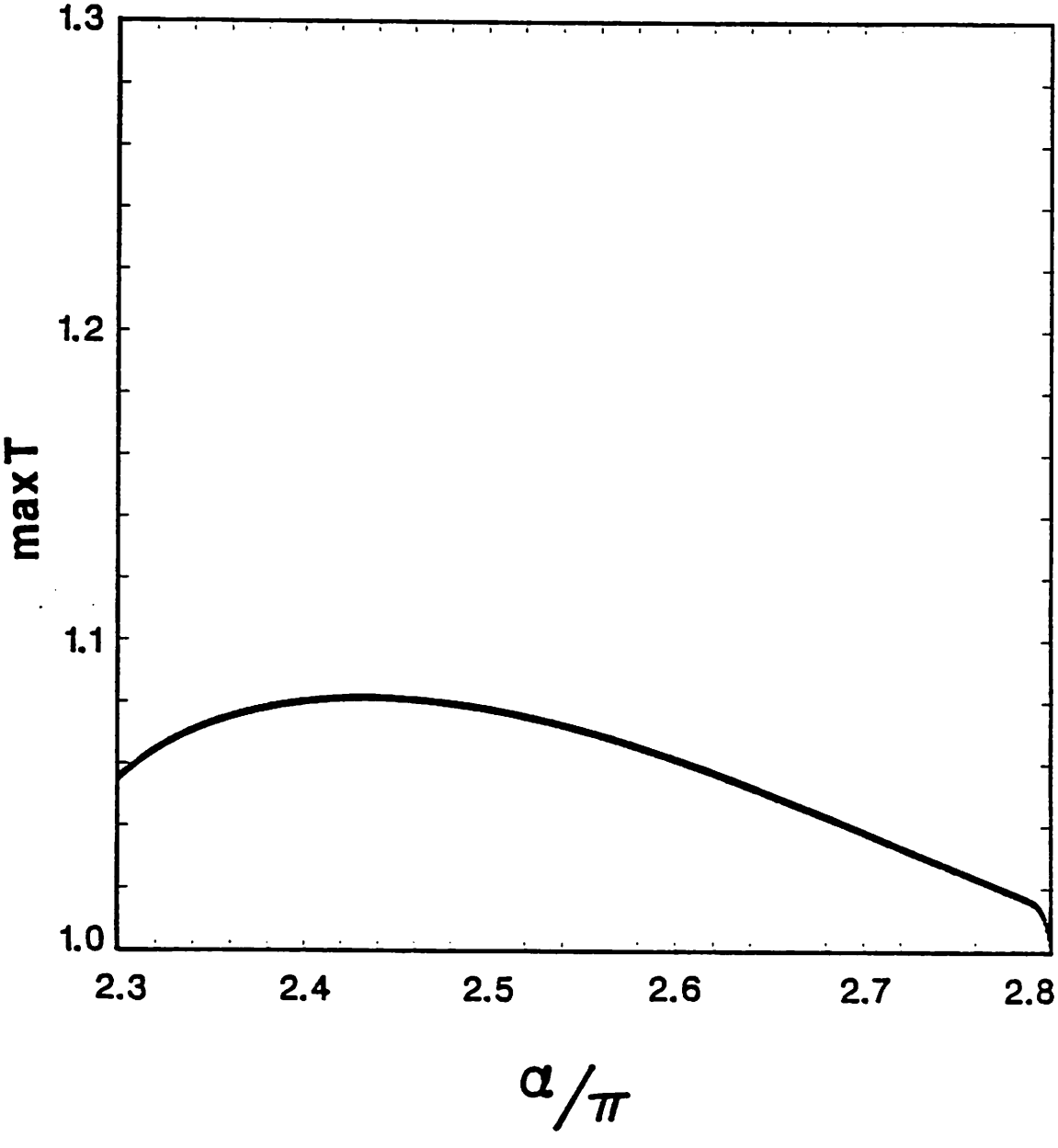

Fig. 23. Bifurcation diagram for $C = 5$

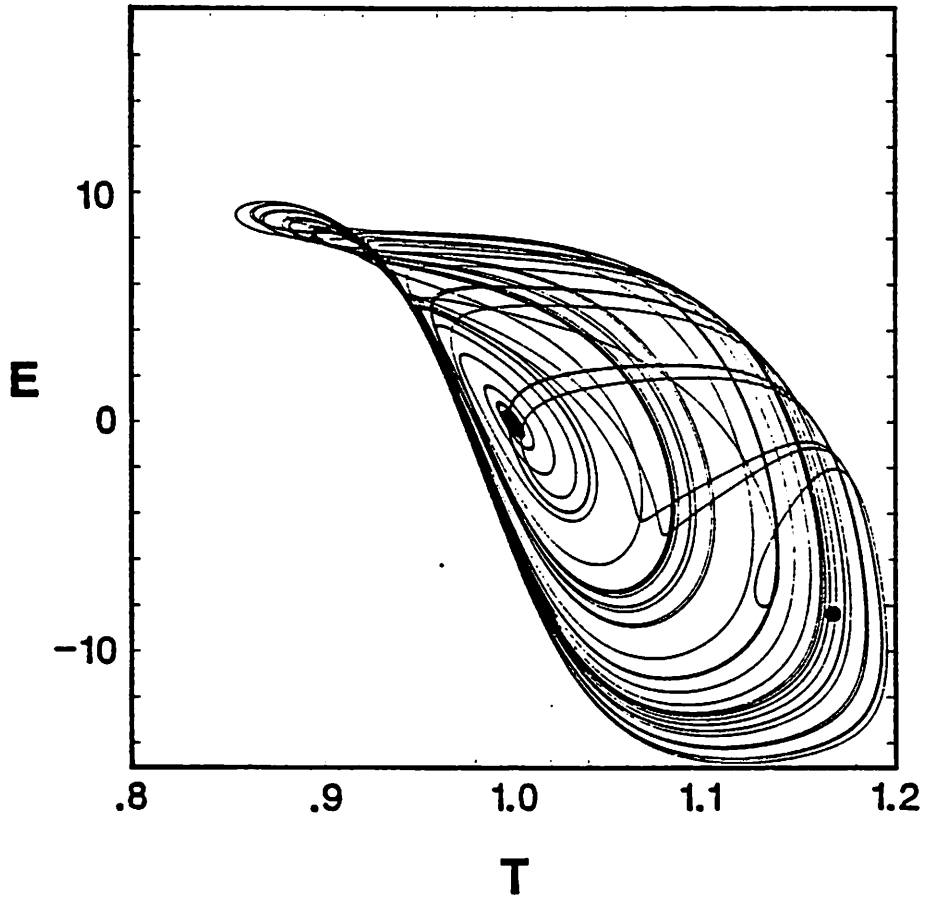

Fig. 24. Orbit trace for $\alpha = 2.758\pi$ and $C = 11$, which is just above the crisis value of α